Journal of Scientific Computing, Vol. 28, Nos. 2/3, September 2006 (© 2006)
DOI: 10.1007/s10915-006-9072-1

Non-Linear PML Equations for Time Dependent Electromagnetics in Three Dimensions

S. Abarbanel,[1] D. Gottlieb,[2] and J. S. Hesthaven[2]

Received April 13, 2005; accepted (in revised form) December 2, 2005; Published online February 23, 2006

In this paper we present a new set of non-linear PML equations for the multi-dimensional Maxwell's equation and show that they are strongly well posed and temporally stable. Numerical examples demonstrate the validity of the new method.

KEY WORDS: Perfectly matched layer; electromagnetics; Maxwell's equations; absorbing boundary conditions.

1. INTRODUCTION

The PML method of Berenger [2], and unsplit variants of it, has become very popular for use in computational electromagnetics (CEM). (See e.g., Turkel and Yefet [9] or Gedney [4] in [8]). The various methods have several features in common, the most prominent of which is the introduction of non-physical variables. This increases the number equations, in the three-dimensional (3D) case, from 6 to 12. Also, at least theoretically [1], they are susceptible to long time temporal growth. While the original Berenger PML equations are only weakly well posed, the other unsplit variants are strongly well posed hyperbolic systems.

In this paper we introduce a new set of PML equations which has a number of features:

1. No non-physical variables are introduced – hence the number of equations is the same as in Maxwell's equations (6 in 3D).

[1] Department of Applied Mathematics, Tel Aviv University, Tel Aviv, Israel.
[2] Division of Applied Mathematics, Brown University, Providence, RI 02912, USA. E-mail: Jan.Hesthaven@Brown.edu

2. The undifferentiated "source-terms" on the right-hand-side of the new equations are algebraically non-linear.
3. The new system has a decaying energy integral and hence the solution is temporally stable.
4. The system is strongly well posed and in particular possesses a unique solution.

In Sec. 2 we present the new set of non-linear PML equations and prove that they possess the properties listed above. In addition, the way the non-linear source terms are derived guarantees that individual plane waves will decay in all direction inside the PML. A slightly different version (identical in 2D but not in 3D) with similar properties is also presented at the end of Sec. 2. In Section 3 we present a few numerical results in two-dimensions (2D) to demonstrate the validity and efficiency of this approach.

2. THE NON-LINEAR PML EQUATIONS

We start by considering the 3D dimensionless Maxwell's equations in vacuum in the absence of currents and charges

$$\frac{\partial \vec{E}}{\partial t} = \nabla \times \vec{H}, \tag{2.1}$$

$$\frac{\partial \vec{H}}{\partial t} = -\nabla \times \vec{E}. \tag{2.2}$$

The non-dimensionalization is similar to that in [1]. This set of equations has a plane-wave solution of the form

$$\vec{E} = \vec{e} I \tag{2.3}$$

$$\vec{H} = \vec{h} I \tag{2.4}$$

where

$$I = \exp[i(\omega t - \vec{k} \cdot \vec{r})] \tag{2.5}$$

with $\vec{r} = (x_1, x_2, x_3)$. Here $\vec{k} = \omega \vec{\alpha}$ is the wave vector and $\vec{\alpha} = (\alpha_1, \alpha_2, \alpha_3)$ is the direction of the propagation. In particular, from Eqs. (2.1) and (2.2) the coefficient vector $(\vec{e}, \vec{h})$ of the plane-wave solution satisfies

$$\vec{e} = -\vec{\alpha} \times \vec{h} \tag{2.6}$$

$$\vec{h} = \vec{\alpha} \times \vec{e}. \tag{2.7}$$

From Eqs. (2.6) and (2.7) one gets, using vector identities,

$$\vec{\alpha} = \frac{\vec{e} \times \vec{h}}{|\vec{h}|^2} = \frac{\vec{e} \times \vec{h}}{|\vec{e}|^2} = \frac{\vec{e} \times \vec{h}}{a|\vec{h}|^2 + (1-a)|\vec{e}|^2}. \tag{2.8}$$

Note that in any given particular direction $\vec{\alpha}$, the coefficient vector $(\vec{e}, \vec{h})$ of the plane wave solution is a linear combination of two linearly independent eigenvectors of Eqs. (2.1) and (2.2). The components of these eigenvectors are functions of the components of $\vec{\alpha}$.

As in the classic PML approach, we surround the computational domain with a PML region and seek equations that cause the electromagnetic field to decay inside the PML region (in any direction of propagation). In this particular work we furthermore seek a set of equations with the following properties:

(i) The total number of equations in the PML should not exceed the number of Maxwell's equations (6 in 3D).
(ii) A monochromatic plane wave in a given direction, upon entering the PML, will decay (in all directions) spatially.
(iii) The energy integral of the solution is temporally stable.
(iv) The system is strongly well posed as an initial value problem in the sense of Gustafsson *et al.* [5].

The above requirements are satisfied by the following set of equations, given here in vector form

$$\frac{\partial \vec{E}}{\partial t} = \left[\nabla + (\vec{\sigma} \otimes \vec{P_H})\right] \times \vec{H} \tag{2.9}$$

$$\frac{\partial \vec{H}}{\partial t} = -\left[\nabla + (\vec{\sigma} \otimes \vec{P_E})\right] \times \vec{E} \tag{2.10}$$

where $\otimes$ stands for the "vector direct product"

$$\vec{a} \otimes \vec{b} = (a_1 b_1, a_2 b_2, a_3 b_3), \tag{2.11}$$

and

$$\vec{P_H} = \frac{\vec{E} \times \vec{H}}{a|\vec{H} \cdot \vec{H}| + (1-a)|\vec{E} \cdot \vec{E}|} \tag{2.12}$$

$$\vec{P_E} = -\frac{\vec{E} \times \vec{H}}{a|\vec{E} \cdot \vec{E}| + (1-a)|\vec{H} \cdot \vec{H}|} \tag{2.13}$$

$$\vec{\sigma} = (\sigma_1(x_1), \sigma_2(x_2), \sigma_3(x_3)) \geqslant 0. \tag{2.14}$$

Note that due to the definitions of $\vec{P}_H$ and $\vec{P}_E$, Eqs. (2.9) and (2.10) contain non-linear undifferentiated terms. Equations (2.9) and (2.10) in detailed component form are shown in Appendix I for both the 2D and 3D cases.

It is readily verified that the following decaying plane wave vector-function $(\vec{E}_A, \vec{H}_A)$, is a solution of Eqs. (2.9) and (2.10):

$$\vec{E}_A = \vec{e} I \cdot e^{-\alpha_1 \int \sigma_1(x_1)dx_1 - \alpha_2 \int \sigma_2(x_2)dx_2 - \alpha_3 \int \sigma_3(x_3)dx_3} \tag{2.15}$$

$$\vec{H}_A = \vec{h} I \cdot e^{-\alpha_1 \int \sigma_1(x_1)dx_1 - \alpha_2 \int \sigma_2(x_2)dx_2 - \alpha_3 \int \sigma_3(x_3)dx_3} \tag{2.16}$$

The subscript A indicates that these are fields assumed for our ansatz.

Here $\vec{e}, \vec{h}$ and $\vec{\alpha}$ are given by Eqs. (2.6), (2.7) and (2.8). Note that for the ansatz (2.15), (2.16)

$$\vec{P_H} = -\vec{P_E} = \vec{\alpha}. \tag{2.17}$$

This is not true in general, and therefore they should be retained as separate entities when solving (2.9), (2.10).

So far we have demonstrated that requirements (i) and (ii) are fulfilled (see (2.9), (2.10) and (2.15), (2.16)). Next we'll show that the solution $(\vec{E}, \vec{H})$ of (2.9), (2.10) is temporally stable. Referring to (2.9), (2.10) we write:

$$\frac{1}{2}\frac{\partial}{\partial t}(\vec{E}\cdot\vec{E}) = \vec{E}\cdot(\nabla\times\vec{H}) + \vec{E}\cdot\left[\vec{\sigma}\otimes\vec{P_H}\right]\times\vec{H} \tag{2.18}$$

$$\frac{1}{2}\frac{\partial}{\partial t}(\vec{H}\cdot\vec{H}) = -\vec{H}(\nabla\times\vec{E}) - \vec{H}\left[\vec{\sigma}\otimes\vec{P_E}\right]\times\vec{E} \tag{2.19}$$

Adding (2.18) and (2.19) we have, using (2.12), (2.13),

$$\begin{aligned}\frac{1}{2}\frac{\partial}{\partial t}(\vec{E}\cdot\vec{E}+\vec{H}\cdot\vec{H}) &= \vec{E}\cdot(\nabla\times\vec{H}) - \vec{H}\cdot(\nabla\times\vec{E}) \\ &\quad -(\vec{\sigma}\otimes\vec{P_H})\cdot(\vec{E}\times\vec{H}) - (\vec{\sigma}\otimes\vec{P_E})\cdot(\vec{E}) \\ &= -\mathrm{div}(\vec{E}\times\vec{H}) - (\vec{\sigma}\otimes\vec{P_H})\cdot\left[(\vec{H}\cdot\vec{H})\vec{P_H}\right] \\ &\quad -(\vec{\sigma}\otimes\vec{P_E})\cdot\left[(\vec{E}\cdot\vec{E})\vec{P_E}\right] \\ &= -\mathrm{div}(\vec{E}\times\vec{H}) - \sum_{i=1}^{3}\sigma_i(\vec{P_{H_i}})^2|\vec{H}|^2 - \sum_{i=1}^{3}\sigma_i(\vec{P_{E_i}})^2|E|^2.\end{aligned} \tag{2.20}$$

Next we take the volume integral of Eq. (2.20), and use the divergence theorem

$$\int \operatorname{div}(\vec{E}\times\vec{H})dV = \int (\vec{E}\times\vec{H})\cdot d\vec{S} = 0, \tag{2.21}$$

such that

$$\frac{1}{2}\frac{d}{dt}\int (|\vec{E}|^2+|\vec{H}|^2)dV = -\sum_{i=1}^{3}\int \sigma_i |P_{H_i}|^2|\vec{H}|^2 dV - \sum_{i=1}^{3}\int \sigma_i |P_{E_i}|^2|\vec{E}|^2 dV < 0. \tag{2.22}$$

Thus the "energy" decays and the solution is temporally stable. The non-linear terms in (2.9), (2.10) $((\vec{\sigma}\otimes\vec{P}_H)\times\vec{E})$ and $((\vec{\sigma}\otimes\vec{P}_H)\times\vec{H})$ are Lipschitz for $0<a<1$. Thus the boundedness of the solution (see Eq. (2.22)) also ensures uniqueness of the solution. This implies that the problem is strongly well posed in the sense of Gustafsson, *et al.* [5].

With the same ansatz as above (see Eqs. (2.15) and (2.16)) one may derive another set of non-linear PML equations which differ slightly from (2.9), (2.10). As before, one starts with (2.15), (2.16) and shows that this ansatz is also satisfied by the following set of equations

$$\frac{\partial\vec{E}}{\partial t} = \nabla\times\vec{H} - \left(\sum_{j=1}^{3}\sigma_j(x_j)\right)\vec{E} + \vec{\sigma}\otimes\vec{E} + (\vec{\sigma}\otimes\vec{H})\times\vec{P}_H \tag{2.23}$$

$$\frac{\partial\vec{H}}{\partial t} = -\nabla\times\vec{E} - \left(\sum_{j=1}^{3}\sigma_j(x_j)\right)\vec{H} + \vec{\sigma}\otimes\vec{H} - (\vec{\sigma}\otimes\vec{E})\times\vec{P}_E. \tag{2.24}$$

In practice it is convenient to use $a=\frac{1}{2}$ in the definition of $\vec{P}_H$ and $\vec{P}_E$, see (2.8), (2.12), (2.13) as in that case the denominator in (2.12), (2.13) is the simply the local energy which is less likely to vanish than one of the computational components, i.e., taking $a=\frac{1}{2}$ tends to yield a slightly more robust algorithm. Equations (2.23) and (2.24) are given in component form in Appendix II.

It can be shown that if $\vec{E}\cdot\vec{H}=0$ (as is the case in the 2D equations of the TE and TM formulations), then the new set of PML equations, (2.23)–(2.24) is identical with the (2.9)–(2.10) set. This, however, is not true in general in the 3D case.

3. COMPUTATIONAL RESULTS

To study the absorption properties of the non-linear set of PML equations presented in Sec. 2 we have implemented the scheme on a square covered by a uniform non-staggered grid using a 4th order centered finite difference algorithms with 3rd order boundary closure. A multidomain approach is used to separate the PML region from the vacuum region. The advancement in time is done using a 4th order Runge–Kutta schemes. The time step, Δt, is chosen to be well below the stability limit although this was done to control temporal errors rather than for stability reasons. No additional dissipation or filtering terms are used in the present work. More details on the computational scheme can be found in [6, 7].

In the numerical tests we first consider the case of continuous excitation applied to the transverse magnetic version of the PML equations (see Appendix A) (A.10)–(A.12). This is done by adding the following forcing terms to (A.8):

$$\begin{pmatrix} H_x^f \\ H_y^f \\ E_z^f \end{pmatrix} = \begin{pmatrix} 0 \\ 0 \\ 1 \end{pmatrix} e^{-ln2\frac{(x-x_a)^2+(y-y_a)^2}{\delta_a}} \sin\left(\frac{\pi t}{10}\right), \tag{3.1}$$

where (x_a, y_a) is the location of the center of the source with width δ_a. The profiles $\sigma_1(x)$, $\sigma_2(y)$ which appear in (A.10)–(A.12) are chosen as

$$\sigma_1(x) = \begin{cases} 0 & |x| \leqslant L \\ c_1 \left(\frac{|x-L|}{\delta_x}\right)^n & L < |x| < L + \delta_x \end{cases}$$

$$\sigma_2(y) = \begin{cases} 0 & |y| \leqslant L \\ c_2 \left(\frac{|y-L|}{\delta_y}\right)^n & L < |y| < L + \delta_y \end{cases}$$

where we have taken a square computational domain bounded by $|x| < L$, $|y| < L$ while δ_x and δ_y refer to the width of the absorbing layer perpendicular to the x and y directions, respectively. The constants c_1, c_2 and n control the shape of the absorbing function inside the layers. We have chosen these parameters to be $c_1 = c_2 = 1$ and $n = 2$. It should be noted that no effort has been made to optimize with respect to c_1, c_2, n, δ_x and δ_y, since the goal of this paper is to present a new approach to deriving "compact" PML systems rather than present a specific and optimized algorithm.

The careful reader will observe that the expression (2.12), (2.13) may result in problems when the fields become very small, rendering the denominator close to zero. This could happen both for zero initial conditions or could be expected to happen deep inside the PML if the layer

does a good job in damping the fields. We have experimented with several ways of addressing this with the simplest and most efficient being to modify (2.12), (2.13) as

$$\vec{P}_H = \frac{\vec{E} \times \vec{H}}{a|\vec{H} \cdot \vec{H}| + (1-a)|\vec{E} \cdot \vec{E}| + \varepsilon} \tag{3.2}$$

$$\vec{P}_E = -\frac{\vec{E} \times \vec{H}}{a|\vec{E} \cdot \vec{E}| + (1-a)|\vec{H} \cdot \vec{H}| + \varepsilon} \tag{3.3}$$

where ε is taken to be of the order of the truncation error or slightly larger. However, thorough computational experiments have shown that taking this factor too large does not seem to impact the accuracy of the PML.

We consider the computational domain $(x, y) \in [-50, 50]$ surrounded (in the non-periodic 2D case) by absorbing layers with width $\delta_x = \delta_y = 10$. The PML in the corner regions is obtained by adding an x and y layer. (We will also show a periodic 2D case with periodic boundary conditions in the y-direction, in that case $\sigma_2(y) = 0$ and $\delta_y = 0$). The forcing source is located at $(x_a, y_a) = (-25, -25)$ with $\delta_a = 3$. The absorbing layers are terminated using characteristic boundary conditions.

The reference solution, with respect to which we inspect the computational results, is a numerical solution of the same problem over a much larger domain of $(x, y) \in [-150, 150]$ but with the same grid spacing throughout. It is easy to show (with the non-dimensional speed of light, $c = 1$) that for $t < 225$ no reflections from the outer boundaries will have sufficient time to propagate back and interact with the solution within $[-50, 50]$. Since we use the exact same algorithm for solving the large (reference) problem and the problem of interest ($(x, y) \in [-50, 50]$) then when we subtract one from the other the truncation errors of the scheme are eliminated. Thus the difference between the two computations may be claimed to represent only the error due to reflections.

The second case we tested was that of an initial pulse which is then being evolved in time by the Maxwell operator. The initial conditions are given by

$$\begin{pmatrix} H_x \\ H_y \\ E_z \end{pmatrix} = \begin{pmatrix} 0 \\ 0 \\ 1 \end{pmatrix} e^{-ln2 \frac{(x-x_a)^2 + (y-y_a)^2}{\delta_a}}. \tag{3.4}$$

All the relevant parameters used in solving Eq. (A.8) are the same as those taken in the case of continuous excitation.

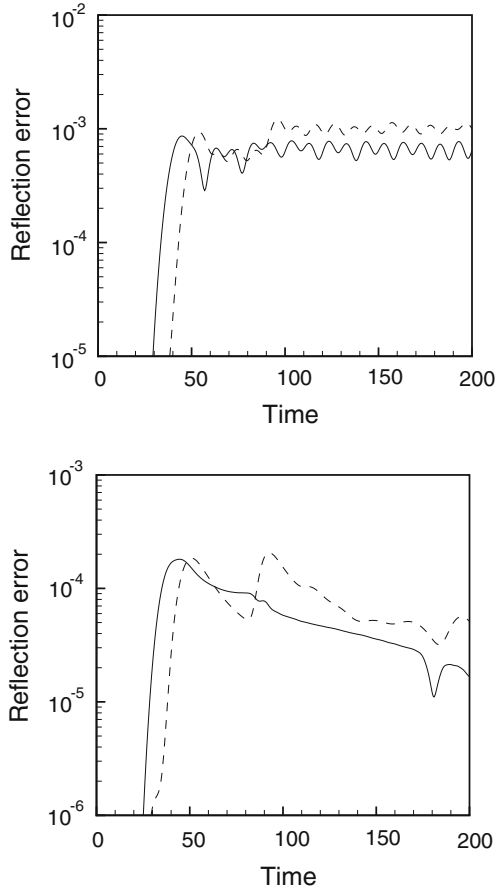

Fig. 1. The L_2 error of H_x (at $x = -48$) for the periodic 2D case with a continuous forcing source (a) as well as for the initial pulse case (b). The solid line represents the results of using the non-linear algorithm while the dashed line represents the computations done using the scheme due to Gedney [3].

In all the cases computed herein (for both the continuous excitation and the initial pulse cases) we calculated the errors of both the present non-linear PML equations and those due to the PML system presented by Gedney [3]. The errors are the L_2 errors along the lines $x = -48$ and $x = 48$ and they were computed as function of time. It turns out that the behavior of the errors of H_x, H_y and E_z are all very similar both in magnitude and time evolution. They are also quite similar at $x = -48$ and $x = 48$. Therefore, in order to reduce the number of figures we show only the L_2 error

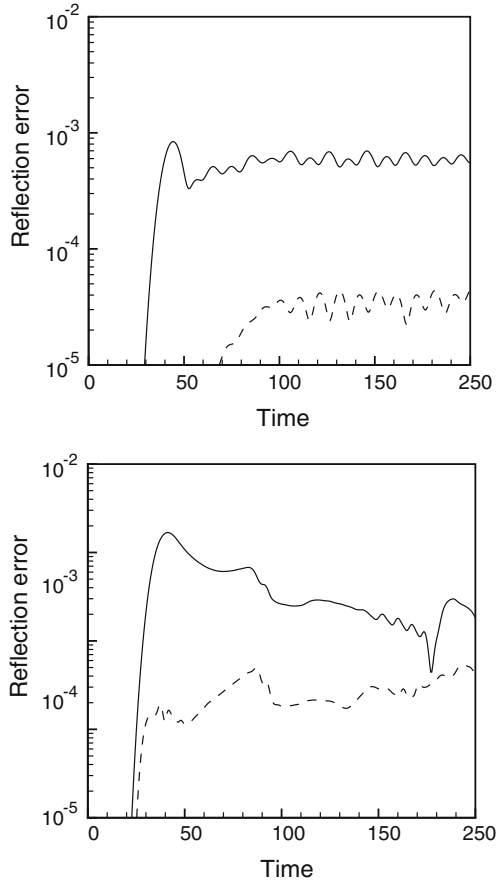

Fig. 2. The L_2 error of H_x (at $x = -48$) for the full 2D case with a continuous forcing source (a) as well as for the initial pulse case (b). The solid line represents the results of using the non-linear algorithm while the dashed line represents the computations done using the scheme due to Gedney [3].

of H_x (at $x = -48$) for both the quasi-2D and the 2D case and for a continuous source as well as initial pulse.

Figure 1 shows the L_2 error of H_x (at $x = -48$) for the periodic 2D case, with a continuous forcing source as well as for the initial pulse case. Figure 2 is the same as Fig. 1 but for the full 2D case. In all cases the solid line represents the results of using the non-linear algorithm. The dashed line represents the computations done using the scheme due to Gedney [3].

We note from Fig. 1 with the continuous source and a periodic 2D configuration that the two algorithms yield quite similar L_2 errors ($\sim 10^{-3}$). For the full 2D case (Fig. 2) the error due to the non-linear PML remains about the same, whereas in the Gedney PML the errors are diminished by an order of magnitude. In the initial pulse cases the non-linear algorithm seems to perform somewhat better in the periodic 2D case. In the 2D case (Fig. 2) again the error due to the Gedney scheme decreases by an order of magnitude whereas the non-linear results remain about the same as in the periodic 2D case. However as time progresses the two error curves approach each other.

Clearly much experimental work remains to be done to determine the sensitivity of the non-linear equations to such parameters as the profiles of σ, the width of the absorbing layers (both in 2D and 3D), and the correct formulation of the PML equations in the overlapping corner regions. We feel that the potential savings in speed and memory size due to the reductions in the number of equations justify exploring these issues further.

APPENDIX A – THE PML EQUATIONS IN COMPONENT FORM (FOR THE CASE $a = \frac{1}{2}$)

In three space dimensions, using $|\vec{H}|^2 = H_1^2 + H_2^2 + H_3^2$ and $|\vec{E}|^2 = E_1^2 + E_2^2 + E_3^2$, the component form of (2.9) and (2.10) is (with $M^2 = \frac{1}{2}(\vec{E}\cdot\vec{E} + \vec{H}\cdot\vec{H})$):

$$\frac{\partial E_1}{\partial t} = \frac{\partial H_3}{\partial y} - \frac{\partial H_2}{\partial z} + \sigma_2(y)\frac{(E_3H_1 - E_1H_3)}{M^2}H_3 + \sigma_3(z)\frac{E_2H_1 - E_1H_2}{M^2}H_2 \tag{A.1}$$

$$\frac{\partial E_2}{\partial t} = \frac{\partial H_1}{\partial z} - \frac{\partial H_3}{\partial x} + \sigma_3(z)\frac{(E_1H_2 - E_2H_1)}{M^2}H_1 + \sigma_1(x)\frac{E_3H_2 - E_2H_3}{M^2}H_3 \tag{A.2}$$

$$\frac{\partial E_3}{\partial t} = \frac{\partial H_2}{\partial x} - \frac{\partial H_1}{\partial y} + \sigma_1(x)\frac{(E_2H_3 - E_3H_2)}{M^2}H_2 + \sigma_2(y)\frac{E_1H_3 - E_3H_1}{M^2}H_1 \tag{A.3}$$

$$\frac{\partial H_1}{\partial t} = -\frac{\partial E_3}{\partial y} + \frac{\partial E_2}{\partial z} + \sigma_2(y)\frac{(H_3E_1 - H_1E_3)}{M^2}E_3 + \sigma_3(z)\frac{H_2E_1 - H_1E_2}{M^2}E_2 \tag{A.4}$$

$$\frac{\partial H_2}{\partial t} = -\frac{\partial E_1}{\partial z} + \frac{\partial E_3}{\partial x} + \sigma_3(z)\frac{(H_1E_2 - H_2E_1)}{M^2}E_1 + \sigma_1(x)\frac{H_3E_2 - H_2E_3}{M^2}E_3 \tag{A.5}$$

$$\frac{\partial H_3}{\partial t} = -\frac{\partial E_2}{\partial x} + \frac{\partial E_1}{\partial y} + \sigma_1(x)\frac{(H_2E_3 - H_3E_2)}{M^2}E_2 + \sigma_2(y)\frac{H_1E_3 - H_3E_1}{M^2}E_1. \tag{A.6}$$

Next we obtain the 2D equations (for the transverse electric, TE, case) by setting $E_3 = H_1 = H_2 = 0$, $\frac{\partial}{\partial z} = 0$:

$$\begin{aligned}
\frac{\partial E_1}{\partial t} &= \frac{\partial H_3}{\partial y} - \sigma_2(y)E_1 \\
\frac{\partial E_2}{\partial t} &= -\frac{\partial H_3}{\partial x} - \sigma_1(x)E_2 \\
\frac{\partial H_3}{\partial t} &= -\frac{\partial E_2}{\partial x} + \frac{\partial E_1}{\partial y} - \sigma_1(x)\left(\frac{E_2^2}{M^2}\right)H_3 - \sigma_2(y)\frac{E_1^2}{M^2}H_3
\end{aligned} \tag{A.7}$$

For the transverse magnetic, TM, case we set $H_3 = E_1 = E_2 = 0$, $\frac{\partial}{\partial z} = 0$:

$$\begin{aligned}
\frac{\partial E_3}{\partial t} &= \frac{\partial H_2}{\partial x} - \frac{\partial H_1}{\partial y} - \sigma_1(x)\left(\frac{H_2^2}{M^2}\right)E_3 - \sigma_2(y)\left(\frac{H_1^2}{M^2}\right)E_3 \\
\frac{\partial H_1}{\partial t} &= -\frac{\partial E_3}{\partial y} - \sigma_2(y)H_1 \\
\frac{\partial H_2}{\partial t} &= \frac{\partial E_3}{\partial x} - \sigma_1(x)H_2.
\end{aligned} \tag{A.8}$$

APPENDIX B – THE PML EQUATIONS, (2.23)–(2.24), IN COMPONENT FORM (FOR THE CASE $a = \frac{1}{2}$)

In three space dimensions, with M defined as in Appendix I, the component form of (2.23) and (2.24) is:

$$\begin{aligned}
\frac{\partial E_1}{\partial t} = {} & \frac{\partial H_3}{\partial y} - \frac{\partial H_2}{\partial z} - (\sigma_2 + \sigma_3)E_1 \\
& -\sigma_2\left(\frac{E_2H_1 - E_1H_2}{M^2}\right)H_2 - \sigma_3\left(\frac{E_3H_1 - E_1H_3}{M^2}\right)H_3
\end{aligned} \tag{B.1}$$

$$\frac{\partial E_2}{\partial t} = \frac{\partial H_1}{\partial z} - \frac{\partial H_3}{\partial x} - (\sigma_3 + \sigma_1) E_2 - \sigma_3 \left(\frac{E_3 H_2 - E_2 H_3}{M^2} \right) H_3 - \sigma_1 \left(\frac{E_1 H_2 - E_2 H_1}{M^2} \right) H_1 \quad \text{(B.2)}$$

$$\frac{\partial E_3}{\partial t} = \frac{\partial H_2}{\partial x} - \frac{\partial H_1}{\partial y} - (\sigma_1 + \sigma_2) E_3 - \sigma_1 \left(\frac{E_1 H_3 - E_3 H_1}{M^2} \right) H_1 - \sigma_2 \left(\frac{E_2 H_3 - E_3 H_2}{M^2} \right) H_2 \quad \text{(B.3)}$$

$$\frac{\partial H_1}{\partial t} = -\frac{\partial E_3}{\partial y} + \frac{\partial E_2}{\partial z} - (\sigma_2 + \sigma_3) H_1 - \sigma_2 \left(\frac{H_2 E_1 - H_1 E_2}{M^2} \right) E_2 - \sigma_3 \left(\frac{H_3 E_1 - H_1 E_3}{M^2} \right) E_3 \quad \text{(B.4)}$$

$$\frac{\partial H_2}{\partial t} = -\frac{\partial E_1}{\partial z} + \frac{\partial E_3}{\partial x} - (\sigma_3 + \sigma_1) H_2 - \sigma_3 \left(\frac{H_3 E_2 - H_2 E_3}{M^2} \right) E_3 - \sigma_1 \left(\frac{H_1 E_2 - H_2 E_1}{M^2} \right) E_1 \quad \text{(B.5)}$$

$$\frac{\partial H_3}{\partial t} = -\frac{\partial E_2}{\partial x} + \frac{\partial E_1}{\partial y} - (\sigma_1 + \sigma_2) H_3 - \sigma_1 \left(\frac{H_1 E_3 - H_3 E_1}{M^2} \right) E_1 - \sigma_2 \left(\frac{H_2 E_3 - H_3 E_2}{M^2} \right) E_2 \quad \text{(B.6)}$$

The 2D form of (2.23)–(2.24) is identical with that given in Appendix A, as mentioned at the end of Sec. 2.

REFERENCES

1. Abarbanel, S., Gottlieb, D., and Hesthaven, J. S. (2002). Long time behavior of the perfectly matched layer equations in computational electromagnetics. *J. Sci. Comput*. **17**, 405–422.
2. Berenger, J.-P. (1994). A perfectly matched layer for the absorption of electromagnetic waves. *J. Comput. Phys*. **114**, 185–200.
3. Gedney, S. D. (1996). Anisotropic perfectly matched layer-absorbing medium for the truncation of FDTD lattices. *IEEE Trans. Antennas Propagat*. **44**, 1630–1639.
4. Gedney, S. D. (1998). The perfectly matched layer absorbing medium. In Taflove, A. (ed.), *Advances in Computational Electrodynamics*, Artech House, pp. 263–344.
5. Gustafsson, B., Kreiss, H. O., and Oliger, J. (1996). *Time Dependent Problems and Difference Methods*, Wiley & Sons.

6. Hesthaven, J. S., and Jameson, L. (1998). A wavelet optimized adaptive multi-domain method. *J. Comput. Phys*. **145**, 280–296.
7. Hesthaven, J. S. (1998). On the analysis and construction of perfectly matched layers for the linearized euler equations. *J. Comput. Phys*. **142**, 129–147.
8. Taflove, A. (1998). *Advances in Computational Electrodynamics*, Artech House.
9. Turkel, E., and Yefet, A. (1998). Absorbing PML boundary layers for wave-like equations. *Appl. Numer. Math*. **27**, 533–557.